ELSEVIER

Journal of Alloys and Compounds 224 (1995) 184–189

Journal of ALLOYS AND COMPOUNDS

Rare earth and uranium transition metal pnictides with $LaFe_4P_{12}$ structure

Christoph B.H. Evers, Wolfgang Jeitschko, Ludger Boonk, Dieter J. Braun, Thomas Ebel, Udo D. Scholz

Anorganisch-Chemisches Institut, Universität Münster, Wilhelm-Klemm-Str. 8, D-48149 Münster, Germany

Received 8 December 1994

Abstract

The new compounds $NdFe_4Sb_{12}$, $SmFe_4Sb_{12}$, $EuFe_4Sb_{12}$ and $SmRu_4Sb_{12}$ were prepared by reaction of the binary lanthanoid antimonides LnSb or $EuSb_2$ respectively, with the transition metals and antimony in sealed silica tubes. Single-crystal structure refinements of $NdFe_4Sb_{12}$ as well as of the previously reported compounds $EuFe_4P_{12}$, UFe_4P_{12}, $EuRu_4Sb_{12}$ and $NdOs_4Sb_{12}$ led to residuals of $R=0.014$, 0.023, 0.013, 0.025 and 0.042 respectively. Systematic differences in the interatomic distances of $CeFe_4P_{12}$, $EuFe_4P_{12}$ and $ThFe_4P_{12}$ suggest that the Fermi level cuts through a phosphorus–phosphorus antibonding band. The thermal parameters of the rare earth components increase with the size of their transition metal–pnictogen cages. The cell volumes of the $LaFe_4P_{12}$ type pnictides suggest that cerium and europium have intermediate valencies. In agreement with the higher electronegativity of phosphorus, cerium is the most tetravalent in the phosphides and europium is the most divalent in the antimonides.

Keywords: Thermal parameters; Cerium; Europium; Rare earths; Uranium transition metal pnictides

1. Introduction

The skutterudite ($CoAs_3$) structure is formed with all nine combinations of the transition metals (T) cobalt, rhodium and iridium with the pnictogens (Pn) phosphorus, arsenic and antimony [1–3]. This cubic structure $\square Co_4As_{12}$ has a large void $\square$, which is filled by the electropositive components in the ternary compounds with $LaFe_4P_{12}$ structure. This ternary structure is again found for phosphides [4], arsenides [5] and antimonides [6], where the electropositive component is a light rare earth element. In addition, such compounds were also prepared with barium [7] and the actinoids thorium [8] and uranium [9] as the third component. More recently we have reported about seven alkaline earth transition metal antimonides AT_4Sb_{12} with A = Ca, Sr, Ba and T = Fe, Ru, Os [10].

During the last ten years we have refined the crystal structures of several $LaFe_4P_{12}$-type compounds and we have also prepared four new antimonides with this structure. These results were only presented at conferences [11,12]. Here we give a detailed account of this work and we briefly review some systematics of this interesting series of compounds.

2. Sample preparation and lattice constants

Starting materials were turnings of uranium (Merck, nuklearrein), the lanthanoids in metallic form (purity > 99.5%), powders of iron (Merck, reinst), ruthenium (Degussa, > 99.5%), osmium (Johnson Matthey, > 99.9%), red phosphorus (Hoechst-Knapsack, ultrapure), and antimony (Ventron, m2N5). Filings of the lanthanoid metals were prepared under argon. They were annealed with the corresponding amounts of antimony in evacuated sealed silica tubes for two days at 450 °C, followed by five days at 750 °C. The resulting antimonides LnSb (Ln = Nd, Sm) and $EuSb_2$ were ground together with the appropriate amounts of the transition metals and antimony, pressed to pellets, and annealed in evacuated, sealed silica tubes. The best results were obtained with the starting compositions corresponding to Ln:T:Sb = 2:4:13 (Ln = Nd, Sm) or Eu:T:Sb = 2:4:14 respectively. The samarium–iron and

SSDI 0925-8388(95)01540-X

Table 1
Lattice constants of new antimonides with the cubic $LaFe_4P_{12}$ structure [a]

Compound	a (pm)	Cell volume (nm^3)
$NdFe_4Sb_{12}$	913.0(1)	0.7610
$SmFe_4Sb_{12}$	913.0(2)	0.7610
$EuFe_4Sb_{12}$	916.5(1)	0.7698
$SmRu_4Sb_{12}$	925.9(1)	0.7938

[a] Standard deviations are given in parentheses in the place values of the least significant digits throughout the paper.

the samarium–ruthenium antimonides have a limited thermal stability range. The corresponding samples were quickly heated to 640 and 600 °C respectively, kept at this temperature for 24 h and quenched. The other samples were quickly heated to 660 °C, kept at this temperature for 3 h, cooled at 1 °C h^{-1} to 600 °C and quenched in water. The excess antimony and lanthanoid antimonides were removed by treating the products with concentrated hydrochloric acid for several days. After this procedure the ternary antimonides were about 90% single phase with the binary transition metal antimonides as impurities.

Well-developed crystals of the phosphides $EuFe_4P_{12}$ and UFe_4P_{12} were obtained from tin melts (tin purity >99.9%). The elements were mixed in the ratio Eu/U:Fe:P:Sn = 1:4:20:50, sealed in evacuated silica tubes, and annealed for one week at 800 °C. After slow cooling (10 °C h^{-1}) the samples were treated with slightly diluted (1:1) hydrochloric acid to dissolve the tin matrix.

All samples are stable in air for long periods of time. They are grey with some metallic lustre. The lattice constants of the new ternary antimonides with $LaFe_4P_{12}$ structure (Table 1) were determined by least-squares fits of the Guinier powder data ($CuK\alpha_1$ radiation) using α-quartz ($a = 491.30$ pm, $c = 540.46$ pm) as an internal standard.

3. Structure refinements

Single crystals of $EuFe_4P_{12}$, UFe_4P_{12}, $NdFe_4Sb_{12}$, $EuRu_4Sb_{12}$ and $NdOs_4Sb_{12}$, isolated from the polycrystalline samples, were investigated with Buerger precession cameras to establish their suitability for the intensity data collections. These data were recorded on four-circle diffractometers with graphite-monochromated Mo or $AgK\alpha$ radiation, respectively (Table 2), using scintillation counters with pulse-height discrimination. The background counts were taken at both ends of each $\theta/2\theta$ scan. Empirical absorption corrections were applied from psi scan data.

The structures were refined by full-matrix least-squares programs with atomic scattering factors [13], corrected for anomalous dispersion [14]. Parameters correcting for isotropic secondary extinction were varied as least-squares parameters. The weights consisted of a constant and a term that accounted for the counting statistics. As checks for the compositions we refined occupancy parameters for all five compounds together with the thermal parameters, while the scale factors were held constant. The resulting occupancy parameters were within three standard deviations at the ideal values with the exception of those for some A sites and the phosphorus position of $EuFe_4P_{12}$. This latter parameter had a value of 0.964(3). Nevertheless, in the final least-squares cycles we assumed the ideal value also for this parameter, because we had never observed a partial occupancy of a phosphorus site in a polyphosphide and since the deviation from the ideal occupancy was small (although seemingly significant with 12σ off the ideal value). The situation is different for the A position, since binary skutterudite compounds TPn_3 are known (albeit with different T components), where this site is unoccupied, and furthermore some compounds were reported [15] with partial occupancy of that site, e.g. $La_{0.20(1)}Co_4P_{12}$ and $Ce_{0.25(1)}Co_4P_{12}$. In the final cycles we therefore varied the occupancy parameters of the A positions when there had been significant deviations in the previous refinement cycles. The resulting atomic parameters and interatomic distances are given in Tables 3 and 4. Listings of the observed and calculated structure factors are available from the authors.

4. Discussion

In the body-centered cubic $LaFe_4P_{12}$ type structure of the compounds AT_4Pn_{12} (Fig. 1) the A atoms are surrounded by 12 Pn atoms and eight T atoms at a somewhat greater distance. Together these 20 atoms form a distorted pentagon dodecahedron (Fig. 2). The T atoms have (distorted) octahedral Pn coordination with two additional A atoms capping two opposite trigonal faces of the octahedra. Each Pn atom has two strongly bonded Pn and two T neighbors forming a distorted tetrahedron. In addition they have one A and four Pn neighbors, which are further away (Table 4).

Chemical bonding in the binary skutterudite phases, e.g. CoP_3, can be rationalized by a simple model [4,16,17], where two electrons are counted for each short (more or less covalent) near-neighbor interaction and where each atom fully uses all bonding orbitals, i.e. the cobalt and the phosphorus atoms obey the 18- and 8-electron rules respectively. In agreement with this model, CoP_3 is a diamagnetic semiconductor, while NiP_3 is believed to be a metallic conductor [18]. This model also roughly allows us to rationalize some properties of the "filled" skutterudites with $LaFe_4P_{12}$ structure: e.g. $Ce^{4+}[Fe_4P_{12}]^{4-}$ — with a polyanion, which

Table 2
Details of the X-ray data collections and the structure refinements of the cubic $LaFe_4P_{12}$ pnictides

	$EuFe_4P_{12}$	UFe_4P_{12}	$NdFe_4Sb_{12}$	$EuRu_4Sb_{12}$	$NdOs_4Sb_{12}$
Space group	$Im\bar{3}$	$Im\bar{3}$	$Im\bar{3}$	$Im\bar{3}$	$Im\bar{3}$
Lattice constant (4-circle diffr.) [a], pm	$a=780.41(1)$	$a=775.5(1)$	$a=912.9(1)$	$a=928.4(2)$	$a=930.0(1)$
Lattice constant (powder), pm	$a=780.55(11)$	$a=777.1(1)$	$a=913.0(1)$	$a=928.2(1)$	$a=929.9(1)$
Formula units/cell	$Z=2$	$Z=2$	$Z=2$	$Z=2$	$Z=2$
Formula weight	746	833	1829	2017	2003
Calculated density, g cm^{-3}	2.61	5.93	7.98	8.37	9.77
Crystal dimensions, μm^3	75·75·75	50·50·50	50·50·50	75·50·50	113·100·63
Radiation	Mo Kα	Mo Kα	Mo Kα	Mo Kα	Ag Kα
Maximal 2θ	65°	80°	65°	75°	55°
Range in h, k, l	−4+16, −4+16, −4+16	±14, ±14, ±14	±13, 0+13, 0+13	0+15, 0+15, ±15	±16, 0+16, 0+16
Total number of reflections	1774	5774	1471	2301	2622
Number of unique reflections	498	283	268	404	450
Reflections with $I_0>3\sigma(I_0)$	323	251	116	163	417
Variable parameters	11	12	12	12	11
Conventional residual	$R=0.023$	$R=0.013$	$R=0.014$	$R=0.025$	$R=0.042$
Weighted residual	$R_w=0.030$	$R_w=0.017$	$R_w=0.015$	$R_w=0.026$	$R_w=0.04$

[a] These lattice constants were obtained on the four-circle diffractometer. They are generally found to be somewhat too small when compared to those refined from the powder data. This is due to systematic errors from absorption, which shifts the diffracted beams to higher angles of the four-circle diffractometer. Therefore, for the calculations of the interatomic distances the lattice constants obtained from the Guinier powder patterns were used.

Table 3
Atomic parameters of $EuFe_4P_{12}$, UFe_4P_{12}, $NdFe_4Sb_{12}$, $EuRu_4Sb_{12}$, and $NdOs_4Sb_{12}$ [a]

Atom	occup.	x	y	z	U_{11}	U_{22}	U_{33}	U_{12}	U_{13}	U_{23}	B_{eq} (Å^2)
$EuFe_4P_{12}$											
Eu	1	0	0	0	50.4(5)	U_{11}	U_{11}	0	0	0	0.398(1)
Fe	1	1/4	1/4	1/4	23.1(6)	U_{11}	U_{11}	2.4(7)	U_{12}	U_{12}	0.183(1)
P	1	0	0.35374(8)	0.14897(8)	38(2)	39(2)	41(2)	0	0	−1(1)	0.310(7)
UFe_4P_{12}											
U	0.947(1)	0	0	0	66.2(5)	U_{11}	U_{11}	0	0	0	0.522(1)
Fe	1	1/4	1/4	1/4	27.9(8)	U_{11}	U_{11}	3(1)	U_{12}	U_{12}	0.220(2)
P	1	0	0.3508(8)	0.1495(8)	37(2)	44(2)	48(3)	0	0	3(2)	0.339(8)
$NdFe_4Sb_{12}$											
Nd	0.832(7)	0	0	0	250(6)	U_{11}	U_{11}	0	0	0	1.97(2)
Fe	1	1/4	1/4	1/4	42(4)	U_{11}	U_{11}	3(5)	U_{12}	U_{12}	0.330(8)
Sb	1	0	0.33575(7)	0.15999(7)	47(2)	92(2)	63(2)	0	0	7(3)	0.534(8)
$EuRu_4Sb_{12}$											
Eu	0.972(9)	0	0	0	149(6)	U_{11}	U_{11}	0	0	0	1.18(1)
Ru	1	1/4	1/4	1/4	47(3)	U_{11}	U_{11}	11(4)	U_{12}	U_{12}	0.372(6)
Sb	1	0	0.3428(1)	0.1583(1)	42(3)	88(3)	72(3)	0	0	8(4)	0.53(1)
$NdOs_4Sb_{12}$											
Nd	1	0	0	0	507(9)	U_{11}	U_{11}	0	0	0	4.00(7)
Os	1	1/4	1/4	1/4	44(2)	U_{11}	U_{11}	5(1)	U_{12}	U_{12}	0.354(2)
Sb	1	0	0.34021(5)	0.15591(5)	59(3)	81(3)	42(2)	0	0	10(1)	0.606(2)

[a] The anisotropic thermal parameters (×10^4) are defined by $T=\exp[-2\pi^2\{h^2a^{*2}U_{11}+\ldots+2klb^*c^*U_{23}\}]$.

seems to be isoelectronic with $CoP_3[Co_4P_{12}]$ – is semiconducting [9,17], while the polyanion in $La^{3+}[Fe_4P_{12}]^{3-}$ is electron deficient and consequently the compound is a metallic conductor [17]. The reader is referred to the literature for a more detailed account of this model [4,16,17], which essentially is in agreement with extended Hückel calculations [19]. A difficulty with this model arises through the fact, that other physical properties – especially magnetic susceptibility [9,17,20] and X-ray absorption near-edge spectroscopy data [20] – suggest an intermediate valence for the cerium atoms in $CeFe_4P_{12}$. Thus, the interaction of the A atoms with the three-dimensionally infinite transition metal–pnictogen polyanion – neglected in the simple two-electron bond model as well as in the extended Hückel calculations – seem to be important [17,20]. In the

Table 4
Interatomic distances (pm) in $EuFe_4P_{12}$, UFe_4P_{12}, $NdFe_4Sb_{12}$, $EuRu_4Sb_{12}$ and $NdOs_4Sb_{12}$ [a]

$EuFe_4P_{12}$			
Eu: 12 P	299.6	P: 1 Eu	299.6
8 Fe	338.0	2 Fe	225.5
		1 P	228.3
Fe: 6 P	225.5	1 P	232.5
2 Eu	338.0	4 P	296.9
UFe_4P_{12}			
U: 12 P	296.3	P: 1 U	296.3
8 Fe	336.5	2 Fe	223.6
		1 P	231.9
Fe: 6 P	223.6	1 P	232.4
2 U	336.5	4 P	296.0
$NdFe_4Sb_{12}$			
Nd: 12 Sb	339.6	Sb: 1 Nd	339.6
8 Fe	395.3	2 Fe	254.9
		1 Sb	292.1
Fe: 6 Sb	254.9	1 Sb	299.9
2 Nd	395.3	4 Sb	344.8
$EuRu_4Sb_{12}$			
Eu: 12 Sb	350.5	Sb: 1 Eu	350.5
8 Ru	401.9	2 Ru	261.8
		1 Sb	291.9
Ru: 6 Sb	261.8	1 Sb	293.9
2 Eu	401.9	4 Sb	349.2
$NdOs_4Sb_{12}$			
Nd: 12 Sb	348.0	Sb: 1 Nd	348.0
8 Os	402.7	2 Os	262.2
		1 Sb	290.0
Os: 6 Sb	262.2	1 Sb	297.2
2 Nd	402.7	4 Sb	352.9

[a] All distances shorter than 320 (Eu–, U–, Fe–P), 350 (Eu–, U–Fe; Nd–, Eu–, Fe–, Ru–, Os–Sb) and 410 (Nd–Fe, Eu–Ru, Nd–Os) pm are listed. The standard deviations are all 0.1 pm or less.

present discussion we will focus our attention on the results of the crystallographic work. Some relevant data of the presently reported structure refinements are summarized in Table 5 together with those of previous refinements.

A comparison of the P–P bond lengths allows us to draw conclusions about the occupancy of bonding and antibonding bands. In general, the P–P bond lengths are similar in the various phosphides with $LaFe_4P_{12}$ structure. Small differences might be attributed to "packing" effects resulting from differences in the lattice constants. However, when the lattice constants are nearly the same, any, even small differences in the corresponding bond lengths should reflect differences in the band structures. It can be gathered from Fig. 3 that the cell volumes of $EuFe_4P_{12}$, $CeFe_4P_{12}$ and $ThFe_4P_{12}$ have similar values, yet it is well known that thorium prefers to be tetravalent, while the volume plot indicates mixed or intermediate valencies $Ce^{+4/+3}$ and $Eu^{+3/+2}$ for the lanthanoids in these $LaFe_4P_{12}$ type phosphides. In Table 6 we compare the lattice constants and some relevant interatomic distances

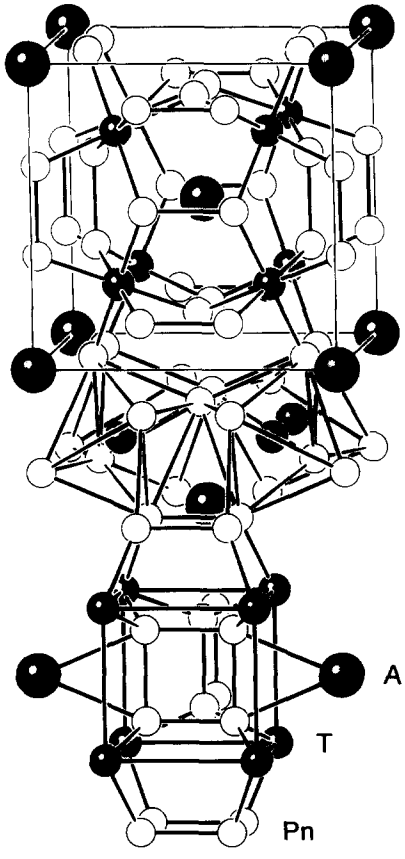

Fig. 1. Crystal structure of the ternary cubic pnictides AT_4Pn_{12} (A = alkaline earth elements, lanthanoids, actinoids; T = Fe, Ru, Os; Pn = P, As, Sb). In the middle of the drawing the TPn_6 octahedra are emphasized; below, the environment of a Pn_4 ring is shown.

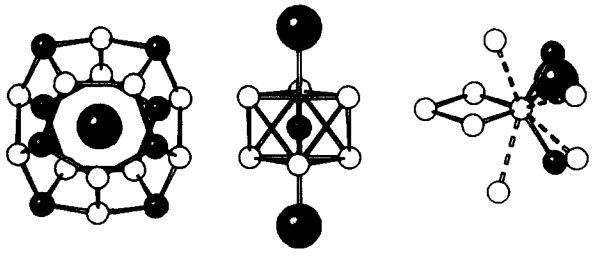

Fig. 2. Near-neighbor coordinations in the $LaFe_4P_{12}$-type structure. The site symmetries of the central atoms are given in parentheses.

of these polyphosphides. As a measure for the similarity of the lattice constants we have listed their ratios in the first row of that table. In the following rows the ratios of some corresponding interatomic distances are given. It can be seen that the lattice constants of the compared compounds are similar, albeit slightly smaller for the compounds with the higher valent A components. This is also the case for most of the interatomic distances. In contrast, the corresponding P–P distances show the reverse tendency, i.e. these distances are larger when the A component has a higher valence. Since phosphorus is the most electronegative component of these com-

Table 5
Lattice constants, positional parameters of the pnictogen atoms, thermal parameters, and the two short pnictogen–pnictogen distances of the compounds AT_4Pn_{12}

Compound AT_4Pn_{12}	Cell constant [pm]	y (Pn)	z (Pn)	B_{eq} [Å^2] (A)	B_{eq} [Å^2] (T)	B_{eq} [Å^2] (Pn)	Pn–Pn distances [a] [pm]		Literature
$LaFe_4P_{12}$	783.16(5)	0.3539(1)	0.1504(1)	0.40(1)	0.24(2)	0.37(2)	228.8	235.6	[4]
$CeFe_4P_{12}$	779.20(10)	0.3522(1)	0.1501(1)	0.42(1)	0.18(2)	0.32(2)	230.4	233.8	[16]
$EuFe_4P_{12}$	780.55(11)	0.35374(8)	0.14897(8)	0.398(1)	0.183(1)	0.310(7)	228.3	232.5	This work
UFe_4P_{12}	777.09(7)	0.3508(8)	0.1495(8)	0.522(1)	0.220(2)	0.339(8)	231.9	232.4	This work
$ThFe_4P_{12}$	779.99(6)	0.3522(1)	0.1508(1)	0.41(1)	0.27(1)	0.39(1)	230.6	235.3	[8]
$LaFe_4As_{12}$	832.52(3)	0.34556(7)	0.15474(7)	0.61(2)	0.24(2)	0.34(2)	257.2	257.7	[5]
$CaFe_4Sb_{12}$	916.2(1)	0.33688(3)	0.15973(3)	2.04(2)	0.424(3)	0.533(3)	298.9	292.7	[10]
$BaFe_4Sb_{12}$	920.0(3)	0.33955(4)	0.16080(4)	0.80(2)	0.51(2)	0.66(1)	295.2	295.9	[7]
$LaFe_4Sb_{12}$	913.95(2)	0.33696(6)	0.16042(5)	1.30(4)	0.24(2)	0.32(2)	298.0	293.2	[6]
$NdFe_4Sb_{12}$	913.0(1)	0.33575(7)	0.15999(7)	1.96(1)	0.313(8)	0.537(8)	299.9	292.1	This work
$SrRu_4Sb_{12}$	928.9(1)	0.34331(6)	015849(6)	1.24(1)	0.407(3)	0.504(6)	291.1	294.4	[10]
$BaRu_4Sb_{12}$	931.5(1)	0.34439(3)	0.15926(3)	0.720(4)	0.342(2)	0.452(3)	289.9	296.7	[10]
$EuRu_4Sb_{12}$	928.24(2)	0.3428(1)	0.1583(1)	1.18(1)	0.372(6)	0.53(1)	291.9	293.9	This work
$NdOs_4Sb_{12}$	929.89(2)	0.34021(5)	0.15591(5)	4.00(7)	0.34(2)	0.60(2)	297.2	290.0	This work

[a] The standard deviations of the Pn–Pn distances are all less than 0.2 pm.

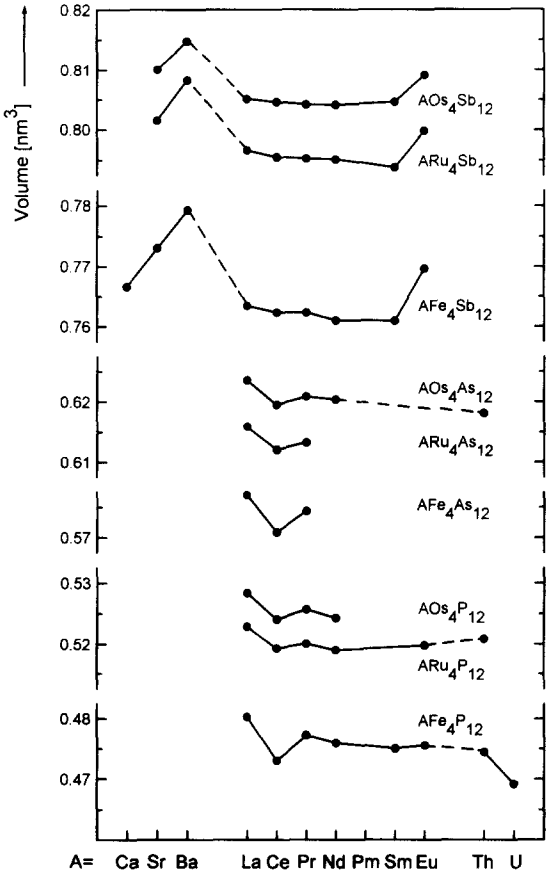

Fig. 3. Cell volumina of $LaFe_4P_{12}$ type compounds.

pounds, the bonding P–P levels can be assumed to lie well below the Fermi level. Hence the stretching of the P–P bonds with increasing electron count of the polyanion may be attributed to the filling of P–P antibonding states. This had briefly been pointed out in comparing the bond distances of $CeFe_4P_{12}$ and $EuFe_4P_{12}$

Table 6
The ratios of the interatomic distances for certain $LaFe_4P_{12}$ type phosphides AFe_4P_{12} with similar lattice constants [a]

	$\frac{CeFe_4P_{12}}{EuFe_4P_{12}}$	$\frac{ThFe_4P_{12}}{EuFe_4P_{12}}$
a	0.9983	0.9993
A–P	0.9957	0.9973
A–Fe	0.9983	0.9993
Fe–P	0.9951	0.9951
P–P	1.0092	1.0101
P–P	1.0056	1.0120

[a] The first row contains the ratios of the lattice constants, in the other rows the ratios of the interatomic distances are listed. The data for $EuFe_4P_{12}$ are taken from the present work, those for $CeFe_4P_{12}$ and $ThFe_4P_{12}$ from [17] and [8] respectively.

[11], and extended Hückel calculations for the $LaFe_4P_{12}$ type compounds showed that indeed the Fermi level cuts through a band, which is highly populated by P–P antibonding states [19].

Another interesting result concerns the thermal parameters of the A atoms. Thermal parameters are frequently affected by errors due to insufficient correction for absorption. In such cases usually the thermal parameters of all atoms are affected in the same way. In our comparison of the thermal parameters of the compounds AT_4Pn_{12}, however, the parameters of the T and the Pn atoms are all similar (Table 5). Therefore the unusually large displacement parameters of some A atoms, especially in the antimonides, are significant. If the transition metal–pnictogen cages of the polyanions are large enough already in the iron phosphides to accommodate the rare earth elements, it can be expected that the A atoms "rattle" in the corresponding arsenides

and antimonides, especially if also the iron atoms are replaced by the larger ruthenium and osmium atoms. Examples which show this effect are $LaFe_4P_{12}$, $LaFe_4As_{12}$ and $LaFe_4Sb_{12}$, where the displacement parameters B_{eq} of the lanthanum atoms increase from 0.40(1) Å^2 in the phosphide over 0.61(2) Å^2 in the arsenide to 1.30(4) Å^2 in the antimonide. The neodymium atoms in $NdOs_4Sb_{12}$ show the largest displacement parameter of $B=4.0(1)$ Å^2. We have investigated this compound by differential scanning calorimetry in the temperature range between −120 and 475 °C. These investigations indicated a displacive-type phase transition both on heating and on cooling at -86 ± 4 °C. However, low-temperature Simon–Guinier powder patterns [21] did not confirm this transition, possibly because the lattice distortion, which may occur during such a phase transition, is too small to be detectable by that method. Similarly, magnetic susceptibility measurements carried out with a SQUID magnetometer [22] did not reveal any discontinuity at this temperature.

The plots of the cell volumes (Fig. 3) show some interesting features. It was already mentioned above that the cerium atoms have a tendency to be tetravalent in $CeFe_4P_{12}$. This tendency decreases in going to the corresponding arsenides and antimonides. Similarly, the cell volumes of the europium compounds deviate the most from the smooth plots for the antimonides and almost do not for the phosphides. Thus, for both the cerium and the europium compounds, the smaller volume (and higher valency) is observed for the phosphides, and the larger volume (lower valency) for the antimonides. This correlates with the higher electronegativity of phosphorus, which favors the higher valency of the A component. There are also some systematics in the cell volumes of the cerium and the europium compounds depending on the transition metal components. Here, however, the tendency is not uniform. For the cerium compounds the higher valency is favored in the iron compounds, while for the europium-containing compounds the higher valency is indicated by the cell volumes of the ruthenium and osmium compounds. Thus, the Fermi level seems to be cutting also through bands involving the transition metal atoms. However, it is difficult to draw conclusions about the relative arrangements of the bands in the various compounds.

Acknowledgments

We thank Mrs. U. Rodewald and Dr. M.H. Möller as well as Prof. Dr. H. Jacobs (Univ. Dortmund) for collecting the various single-crystal diffractometer data sets. Prof. Dr. W. Eysel (Univ. Heidelberg) and Mr. C. Brendel were so kind as to investigate $NdOs_4Sb_{12}$ by difference scanning calorimetry. We also acknowledge generous gifts of platinum metals (Dr. W. Gerhartz, Degussa and Dr. D.T. Thompson, Johnson Matthey) and silica tubes (Dr. G. Höfer, Heraeus Quarzchmelze). This work was supported by the Deutsche Forschungsgemeinschaft and the Fonds der Chemischen Industrie.

References

[1] N.N. Zuravlev and G.S. Zhdanov, *Sov. Phys. Crystallogr., 1* (1956) 404.
[2] S. Rundqvist and N.O. Ersson, *Ark. Kem., 30* (1968) 103.
[3] A. Kjekshus and T. Rakke, *Acta Chem. Scand., A28* (1974) 99.
[4] W. Jeitschko and D.J. Braun, *Acta Crystallogr., B33* (1977) 3401.
[5] D.J. Braun and W. Jeitschko, *J. Solid State Chem., 32* (1980) 357.
[6] D.J. Braun and W. Jeitschko, *J. Less-Common Met., 72* (1980) 147.
[7] N.T. Stetson, S.M. Kauzlarich and H. Hope, *J. Solid State Chem., 91* (1991) 140.
[8] D.J. Braun and W. Jeitschko, *J. Less-Common Met., 76* (1980) 33.
[9] G.P. Meisner, M.S. Torikachvili, K.N. Yang, M.B. Maple and R.P. Guertin, *J. Appl. Phys., 57* (1985) 3073.
[10] C.B.H. Evers, L. Boonk and W. Jeitschko, *Z. Anorg. Allg. Chem., 620* (1994) 1028.
[11] L. Boonk, W. Jeitschko, U.D. Scholz and D.J. Braun, *Z. Kristallogr., 178* (1987) 30.
[12] C.B.H. Evers, W. Jeitschko and L. Boonk, *Z. Kristallogr. Suppl., 5* (1992) 62.
[13] D.T. Cromer and J.B. Mann, *Acta Crystallogr., A24* (1968) 321.
[14] D.T. Cromer and D. Liberman, *J. Chem. Phys., 53* (1970) 1891.
[15] S. Zemni, Duc. Tranqui, P. Chaudouet, R. Madar and J.P. Senateur, *J. Solid State Chem., 65* (1986) 1.
[16] J. Ackermann and A. Wold, *J. Phys. Chem. Solids, 38* (1977) 1013.
[17] F. Grandjean, A. Gérard, D.J. Braun and W. Jeitschko, *J. Phys. Chem. Solids, 45* (1984) 877.
[18] F. Hulliger, *Structure and Bonding, 4* (1968) 83.
[19] D. Jung, M.-H. Whangbo and S. Alvarez, *Inorg. Chem., 29* (1990) 2252.
[20] J.S. Xue, M.R. Antonio, W.T. White, L. Soderholm and S.M. Kauzlarich, *J. Alloys Comp., 207/208* (1994) 161.
[21] A. Simon, *J. Appl. Crystallogr., 4* (1971) 138.
[22] M.E. Danebrock, C.B.H. Evers and W. Jeitschko, unpublished results (1993).